Multi-objective Optimization of Masonry Housing Systems for Sustainable Structural and Thermal Performance

Zarate-Perez, Josue[1]; Huamán-Arauco, Claudia[1]; Zarate-Perez, Eliseo[1]
[1]Universidad Privada del Norte (UPN), Peru, *n00169159@upn.pe, n00092811@upn.pe, eliseo.zarate@upn.edu.pe*

***Abstract*– This study proposes a sustainable, innovative approach to improving the structural resilience and energy performance of low-rise housing in seismic zones. It analyzes the structural and thermal behavior of residential buildings constructed with the two predominant masonry systems in Peru: structural and mixed masonry. Structural simulations were performed using software in accordance with national regulations and under high seismic hazard scenarios. A genetic algorithm (GA) was applied to optimize the design by simultaneously considering seismic stiffness, thermal comfort, and estimated cost criteria. The results show that both systems comply with regulatory drift limits. However, mixed masonry is more rigid and has lower total drift. The GA identified construction configurations that balance structural safety, energy efficiency, and economic viability. These findings contribute to sustainable housing development and support multi-criteria decision-making in emerging economies.**

***Keywords*– Structural optimization, Genetic algorithm, Masonry systems, Seismic performance, Sustainable housing.**

I. INTRODUCTION

The construction industry and energy consumption in residential buildings have contributed significantly to global environmental degradation, resulting in high demand for natural resources and an increase in greenhouse gas emissions. Globally, residential buildings account for a significant proportion of energy consumption and CO_2 emissions, mainly due to indoor climate control, the demand for which has increased because of urban growth and climate change [1]; [2]; [3].

In this context, improving the thermal performance of building envelopes is essential to reduce energy consumption. To achieve this, it is essential to implement innovative materials and sustainable building systems that balance energy efficiency with structural safety, especially in seismically active areas such as Peru.

Peru is in the Pacific Ring of Fire, one of the most seismically active regions on the planet. The subduction of the Nazca plate under the South American plate generates intense tectonic activity, making our country highly vulnerable to earthquakes (IGP, [4], [5], [6], [7]). This reality requires construction solutions that guarantee not only energy efficiency, but also seismic resistance, in accordance with the National Building Code [8].

Several studies have highlighted the importance of building materials in the sustainability of housing [9]; [10]. Among the traditional solutions with potential for improvement are mixed masonry, using King Kong-type clay bricks, and structural masonry, based on reinforced concrete blocks with vertical steel. Both systems have relevant thermal and mechanical properties and use materials with low environmental impact and recycling potential [11]; [12].

Clay bricks have a high thermal mass, which regulates the indoor temperature and reduces the dependence on mechanical air-conditioning systems. Concrete blocks used in structural masonry offer high load-bearing capacity and allow the integration of reinforcements that improve the seismic performance of buildings. These characteristics make them an attractive alternative for low-rise housing in urban areas of the country.

In addition to conventional structural analysis, this study incorporates the use of a Genetic Algorithm (GA) as a multi-criteria optimization tool. This evolutionary technique allows the identification of optimal design configurations that simultaneously consider structural stiffness, thermal performance, and estimated construction cost. By simulating different combinations of design variables, the GA allows the selection of alternatives that balance safety, efficiency, and economic viability.

Therefore, the objective of this work is to comparatively evaluate the structural behavior of residential buildings constructed with mixed masonry and structural masonry. For this purpose, the computer program structural is used to model and analyze both systems according to the parameters established in the Technical Standard E.030, considering modal analysis, lateral displacements, shear forces, interstory drift and structural stiffness. The research focuses on buildings representative of the Peruvian context and addresses the optimization process with GA to contribute to decision-making in sustainable and seismic construction solutions.

II. METHODOLOGY

A. Design of the base building

This research was based on the floor plan of a single-family house representative of the Peruvian context, as shown in Figure 1. The building was modeled with two structural systems: confined masonry and structural masonry, both evaluated according to the National Building Code [8]. Table 1 summarizes the technical specifications of the house model considered. It is a two-story category A house with a floor area of 62 m² and a height of 2 m. It is in seismic zone Z4 of Peru, with a seismic factor of 0.45 and a soil profile type S2, according to Peruvian Technical Standard E.030 [13], which requires special measures to ensure adequate seismic performance.

Fig. 1 Architectural layout of a single-story residential unit.

TABLE I
MODEL BUILDING SPECIFICATIONS

Description	Details
Building Use	Single-family residential – Category A
Total Built Area	62 m²
Number of Floors	2
Materials	Clay, concrete, steel
Seismic Zone	Z4 (0.45) – Standard E.030
Soil Profile	Type S2 – Standard E.030
Total Height	6.2 m
Location	Peru

B. *Characteristics of Materials*

Table 2 shows the mechanical properties of the materials used in each structural system. In the mixed masonry system, 24 cm clay brick perimeter walls were used, reinforced with reinforced concrete columns and beams. The structural masonry used 15 cm concrete blocks with vertical reinforcement of 3/8" steel bars embedded in mortar.

TABLE II
PROPERTIES OF MATERIALS USED IN MASONRY SYSTEMS

System	Material	Size / Classification	Density (kg/m³)	E (GPa)	f' (MPa)
Composite Masonry	Concrete (fc = 210 kg/cm²)	N/A	2400	25	30
	Clay brick	9×12.5×23 cm	2000	15	5
	Steel (9 m rebar)	—	7850	210	350
Structural Masonry	Concrete block	40×20×20 cm	1900	6	6
	Grout	N/A	2200	15	10
	Steel (3/8" rebar)	—	7850	25	30

C. *Structural Analysis in structural*

The structural analysis was performed using the structural software, which uses a three-dimensional model to simulate the dynamic response of the systems. According to the standards E.020 (loads), E.030, [8, 13], the properties of the materials, structural sections, boundary conditions, gravity and seismic loads were defined.

D. *Mixed masonry modeling*

The structural elements (beams, columns and walls) were defined as frame and cladding elements (Fig. 2). The lightweight slabs were modeled as rigid membranes with a thickness of 20 cm. Three types of beams and columns were used Beams: VP (0.24 × 0.40 m), VS (0.24 × 0.20 m), and VCH (0.20 × 0.20 m). Columns: C1 (0.25 × 0.25 m), C2 (0.24 × 0.20 m).

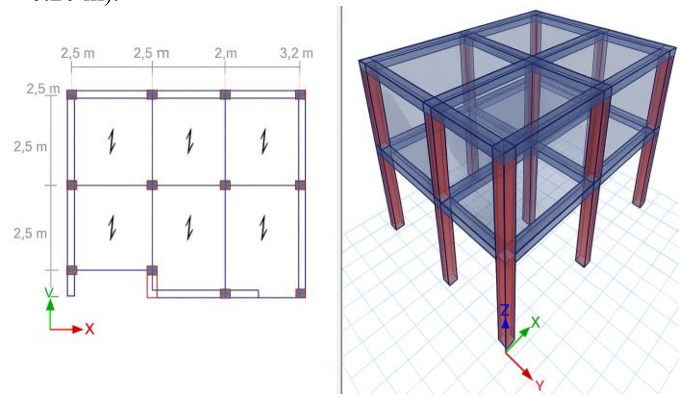

Fig. 2 Composite Masonry Structural Model in structural.

D. *Structural Masonry Modeling*

The load bearing walls were defined as 12 cm shell elements reinforced with 3/8" steel bars from the foundation to the roof. Solid 12 cm slabs and primary (20×40 cm) and secondary (20×20 cm) beams were assigned to distribute the loads. The model was evaluated using modal analysis to verify displacements, displacements, and internal stresses (Fig.3).

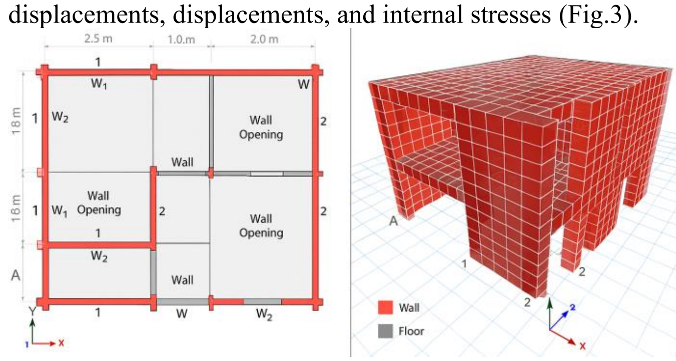

Fig. 3 Magnetization as a function of applied field.

E. *Calculation for Mixed Masonry and Structural Masonry*

This section describes the structural methodology used to model residential buildings with mixed masonry and structural masonry systems. The basic equations for calculating area and moment of inertia are presented, as well as special considerations for reinforcement of bearing walls and rigid diaphragms.

i) Calculation of area and moment of inertia

The structural sections of beams, columns and walls are modeled with rectangular geometry. Equations 1 and 2 are used to determine the cross-sectional area (A) and moment of inertia (I).

$$A = b \ x \ h \tag{1}$$

$$I = \frac{(b \ x \ h^3)}{12} \tag{2}$$

Where b is the width of the section and h is the height. These formulas apply to both framing members (beams and columns) and walls modeled as shells.

ii) Axial and bending stiffness.

The structural stiffness is calculated using equations 3 and 4.

$$EA = E \; x \; A \tag{3}$$

$$EI = E \; x \; I \tag{4}$$

E is the modulus of elasticity, A is the cross-sectional area, and I is the moment of inertia. For concrete, E can be estimated using Equation 5.

$$E = 4700 \; x \sqrt{fc} \tag{5}$$

iii) Specifics of structural masonry.

For reinforced masonry, the contribution of mortar and rebar shall be considered. The equivalent stiffness is calculated using Equation 6.

$$E_{equiv} = \frac{E_m \cdot A_m + E_s \cdot A_s}{A_{total}} \tag{6}$$

E_m and A_m correspond to masonry, E_s and A_s to steel, and A_{total} is the total area of the section.

iv) Rigid diaphragm considerations

In both systems, the lightweight slabs are modeled as rigid diaphragms that distribute lateral loads. In the case of structural masonry, it is important to ensure adequate connection between the wall and the slab.

F. Loads applied

The structural analysis considered the dead load (300 kg/m²), the residential overload (200 kg/m²), and an additional load of 100 kg/m² due to the finishes. Seismic loads were applied using equivalent static and spectral modal analysis, considering 100% of the dead load and 25% of the live load, according to standard E.030 [13]. These loads were distributed using rigid diaphragms at each level of the structural model. Table 3 shows the full details.

TABLE III
CONSIDERED SEISMIC PARAMETERS

Parameter	Symbol	Value
Seismic zone factor	Z	0.45 (Z4)
Building use factor	U	1.50 (Cat. A)
Soil type factor	S	1.05 (S2)
Number of stories	N	2
Floor area	Ap	61.00 m²

G. Genetic algorithm (GA) for multicriteria optimization.

In this study, a simplified genetic algorithm was used as a heuristic search tool for the simultaneous optimization of three performance criteria in building systems: structural stiffness, thermal performance, and estimated construction cost [14]. The procedure was developed in the Python programming language and adapted to the parametric analysis of low-rise residential buildings built in seismic areas.

i) Coding and design variables

Everyone in the population was represented by a vector of four continuous variables, as expressed in Equation 7 [15].

$$X = [\, e, h, s, \lambda] \tag{7}$$

Where e is the wall thickness (m), h is the floor height (m), s is the column section (m), and λ is the thermal conductivity of the enclosure material (W/m-K). These variables were limited to a realistic physical range in accordance with building and code restrictions.

ii) Objective functions.

Three objective functions were defined to be maximized or minimized according to the criteria and are shown in the following equations.

$$f_1(x) = \frac{e \; x \; s}{h} \tag{8}$$

The relative structural stiffness (to be maximized) is expressed in equation 8 [14].

The thermal performance (which should be maximized, i.e. it is inversely proportional to the U-value) is expressed in equation 9 [15].

$$f_2(x) = \frac{1}{e \; x \; \lambda} \tag{9}$$

The estimated construction cost (which should be minimized) is shown in equation 10 [14].

$$f_3(x) = (\, e + s \,) \,.\, h \,.\, C_u \tag{10}$$

Cu represents a unit coefficient for the cost of the material, and USD 150/m³ was used as the base value in the simulation.

iii) Genetic operators

To apply the GA algorithm to optimization, genetic selection, crossover and mutation operators were used. In the case of selection, it was performed by composite fitness, prioritizing individuals with the highest performance in the weighted sum of criteria (fitness). In the case of crossover, the intermediate linear type was applied, as shown in equation 11 [16].

$$X_{hijo} = \propto x \; X_{p1} + (\, 1 - \propto) \; x \; X_{p2} \;\; \propto \; \epsilon \; [0,1] \tag{11}$$

In the case of mutation, the Gaussian additive transformation with probability p_m was applied to each gene, and its application is shown in equation 12 [16].

$$X'_i = X_i + \mathcal{N}(0, \sigma^2) \tag{12}$$

Where N is a normal distribution centered at zero and σ = 0.02.

iv) Evolutionary procedure

The procedure consists in randomly initializing the population P_0 with size N = 50. The fitness of everyone is evaluated using functions f_1, f_2 and f_3, and the best individuals are selected according to their composite fitness, which is given by equation 13 [14].

$$fitness = f_1 + f_2 - \omega x f_3 \tag{13}$$

Where $\omega = 10^{-4}$ is a cost penalty factor.

Finally, new individuals are generated by crossover and mutation, the population is replaced, and the generation proceeds for G = 40 iterations. The final solutions were plotted on a Pareto front graph, where the relationship between structural stiffness, thermal performance, and cost was analyzed. The analysis identified optimal configurations adapted to different design objectives, such as energy efficiency and seismic resistance.

III. RESULTS AND DISCUSSIONS

The comparative analysis of the results obtained for the mixed masonry and structural masonry systems shows significant differences in their dynamic performance under seismic loads (Table IV). In terms of maximum floor drift, the mixed masonry system shows higher values in the Y direction, especially on the second floor, where it reaches a value of

0.00066 (unitless), indicating greater flexibility in this direction. On the other hand, the structural masonry shows lower and more symmetrical displacement values between levels, indicating a more rigid and uniform behavior against lateral actions.

TABLE IV
COMPARISON OF STRUCTURAL PARAMETERS BETWEEN MIXED MASONRY AND STRUCTURAL MASONRY SYSTEMS BY PLANE AND DIRECTION.

	Category (Variable – Unit)	Nivel 1 - X	Nivel 1 - Y	Nivel 2 - X	Nivel 2 - Y
Structural System	Maximum Story Drift – SDX (Drift, Unitless)	0.0001	0.00016	0.00025	0.0004
	Maximum Story Drift – SDY (Drift, Unitless)	0.00013	0.00023	0.00026	0.00066
	Maximum Story Displacement – SDY (Displacement, m)	0.0002	0.0003	0.00045	0.00064
	Maximum Story Displacement – SDX (Displacement, m)	0.0001	0.00015	0.00023	0.00031
	Story Shears – SDX (Force, kgf)	13500	8500	13500	14982
	Story Shears – SDY (Force, kgf)	40000	46000	40000	46623
Structural Masonry	Maximum Story Drift – SDX (Drift, Unitless)	0.0001	7.50E-05	0.000128	0.000128
	Maximum Story Drift – SDY (Drift, Unitless)	0.00015	0.00017	0.000234	0.000234
	Maximum Story Displacement – SDX (Displacement, m)	0.00022	0.00031	0.00064	0.00064
	Maximum Story Displacement – SDY (Displacement, m)	0.00075	0.00135	0.0011	0.00135
	Story Shears – SDX (Force, kgf)	13904	13904	13904	13904
	Story Shears – SDY (Force, kgf)	41479	41479	41479	41479

With respect to the maximum displacement of the floors, the mixed masonry system shows moderate displacements in both directions, with a maximum of 0.00064 m on the second floor in the Y direction. However, the structural masonry system shows significantly higher displacements, reaching up to 0.00135 m in the Y direction. This behavior indicates a greater deformability of the system, despite its good dissipation capacity, which could affect occupant comfort or the integrity of non-structural elements.

In terms of shear forces at the base (Story Shears), the structural masonry system shows a more homogeneous distribution between floors, with constant values in both the X and Y directions (13,904 and 41,479 kgf, respectively). In contrast, the mixed masonry shows a greater variation, especially in the Y direction, where the shear force increases significantly in the second plane. This uneven distribution can lead to the accumulation of stresses that compromise the safety or durability of the system under severe seismic conditions.

Structural masonry provides more robust and symmetrical performance, with better control of drifts and internal stress, albeit with larger absolute displacements. Mixed masonry shows less overall displacement but greater variability in response, so detailed analysis would be required in the design stages to ensure its seismic performance. Both systems are viable for low-rise residential buildings, but their selection will depend on prioritized design criteria such as stiffness, displacement control, or load distribution efficiency.

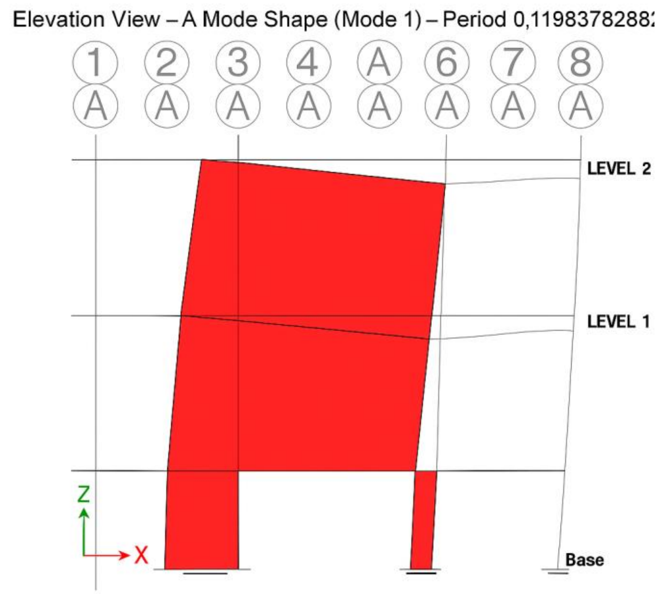

Fig. 4 First Mode of Vibration – Composite Masonry (Period = 0.1198 s).

Figure 4 shows the modal shape corresponding to the mixed masonry structure with a period of 0.1198 s obtained from the modal analysis. The enhanced deformation in the global Y direction is shown, indicating that lateral displacements in this direction have the highest modal contribution. The deformation indicates a predominantly translational behavior, with increasing displacements towards level 2, while the base remains fixed. This representation allows to identify the vulnerability of the system to dynamic loads and is essential to validate its overall stiffness and seismic behavior in the structural analysis.

The first mode of vibration of the structural masonry system has a natural period of 0.1937 s, corresponding to a frequency of 5.16 Hz, indicating a rigid structure with a fast response to seismic excitations. The deformation shows displacements predominantly in the Y-direction with no evidence of significant torsion, suggesting stable and symmetric dynamic behavior. This configuration is favorable for low-rise buildings because it reduces lateral displacements and maintains an efficient distribution of forces (Fig. 5).

The modal analysis of the mixed masonry system shows that the first vibration mode has a period of 0.2 s and a frequency of 5.01 Hz, indicating a relatively rigid structure suitable for low-rise buildings. The first three modes account for most of the dynamic response, with frequencies of 5.01 Hz, 6.46 Hz, and 8.45 Hz, respectively, indicating a harmonic distribution of structural behavior. As the number of modes increases, the periods decrease rapidly (0.061 s, 0.044 s, and 0.036 s), reflecting a greater involvement of modes with local deformations or greater complexity.

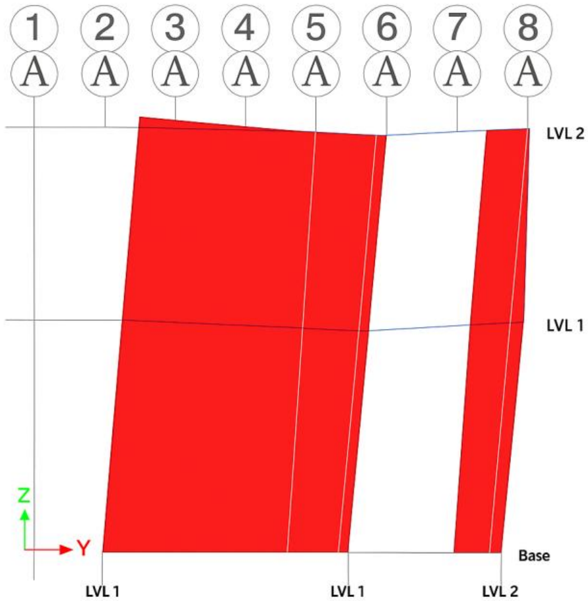

Fig. 5 First Mode of Vibration – Structural Masonry (Period = 0.1937 s).

This modal configuration consists of systems with load-bearing walls and rigid diaphragms, where translational displacements predominate and limited structural bending or torsion occurs. Taken together, these values indicate that the building responds efficiently to seismic loads, with behavior dominated by low-frequency modes and good modal separation.

TABLE V
MODAL PERIODS AND FREQUENCIES – COMPOSITE MASONRY SYSTEM.

Case	Mode	Period	Frequency	CircFreq	Eigenvalue
		sec	cyc/sec	rad/sec	rad²/sec²
Modal	1	0.2	5.007	31.4611	989.8029
Modal	2	0.155	6.456	40.5632	1645.3711
Modal	3	0.118	8.451	53.0996	2819.5677
Modal	4	0.061	16.438	103.282	10667.112
Modal	5	0.044	22.489	141.301	19966.016
Modal	6	0.036	27.929	175.481	30793.472

The analysis of accelerations by level for the mixed masonry system shows that the largest responses are concentrated on the second level, where a maximum acceleration of 517.88 cm/s² is reached under seismic action in the Y-direction (SDY), significantly exceeding that recorded in the X-direction (231.21 cm/s²), shows in Table VI. This behavior is consistent with the dynamic amplification typical of low-rise structures with progressive stiffness. The most significant rotational accelerations are observed in RX (1.409 rad/s²) and RY (0.617 rad/s²), indicating a slight torsional involvement.

Vertical accelerations (UZ) remain below 282 cm/s², indicating a lesser influence of the vertical component of the earthquake. Overall, the results highlight the need to adequately reinforce the structural and non-structural elements of the upper level, where the highest dynamic demands are concentrated.

TABLE VI
STORY ACCELERATIONS – COMPOSITE MASONRY SYSTEM (CM/S² AND RAD/S²).

Story	Output Case	UX	UY	UZ	RX	RY	RZ
		cm/sec²	cm/sec²	cm/sec²	rad/sec²	rad/sec²	rad/sec²
Lev 2	SDX	231.208	130.443	68.826	0.375	0.389	0.277
	SDY	48.842	517.88	281.911	1.409	0.617	0.088
Lev 1	SDX	128.965	72.408	45.711	0.253	0.328	0.152
	SDY	23.763	279.159	182.084	0.905	0.337	0.037
Base	SDX	0	0	0	0.25	0.358	0.009
	SDY	0	0	0	1.21	0.196	0.036

The structural masonry system exhibits a first vibration mode with a period of 0.12 seconds and a corresponding frequency of 8.35 Hz, indicating a structure with high overall stiffness, typical of buildings with load-bearing concrete walls, as shown in Table VII. The higher modes also reflect compact dynamic behavior, with rapidly decreasing periods and frequencies exceeding 10 Hz from the second mode onward. This distribution shows a clear concentration of modal energy in the first modes, suggesting that most of the seismic responses will be dominated by translational displacements, without significant involvement of torsional or local modes. The notable difference between the first and second modes, as well as the high frequency of the third mode (14.69 Hz), reinforces the conclusion that the structure responds to seismic motions in a rapid and controlled manner. This pattern is characteristic of buildings with rigid and massive systems, where modal separation contributes to lower structural resonance amplification.

TABLE VII
MODAL PERIODS AND FREQUENCIES – STRUCTURAL MASONRY SYSTEM.

Case	Mode	Period	Frequency	CircFreq	Eigenvalue
		sec	cyc/sec	rad/sec	rad²/sec²
Modal	1	0.12	8.345	52.4307	2748.98
	2	0.098	10.242	64.3517	4141.14
	3	0.068	14.694	92.3252	8523.93
	4	0.038	26.316	165.351	27340.9
	5	0.034	29.817	187.347	35098.8
	6	0.025	40.35	253.529	64277.1

The Pareto plot (Figure 6) shows the optimal solutions obtained by implementing a simplified genetic algorithm. In this two-dimensional graph, each point represents a unique structural configuration evaluated in terms of its structural stiffness (X-axis) and thermal performance (Y-axis), while the color scale indicates the estimated cost of that solution. This representation allows us to identify alternatives that offer an efficient balance between the three fundamental criteria of sustainable building design.

A partial inverse trend can be observed between stiffness and thermal performance, indicating that improving one criterion tends to compromise the other. Solutions with high stiffness are often associated with more robust structural sections, which increases the volume of materials used and consequently the cost and thermal conductivity of the system. On the other hand, configurations that maximize thermal performance often use thicker walls of low-conductivity materials, which can reduce relative stiffness if the load-bearing sections are not adequately reinforced.

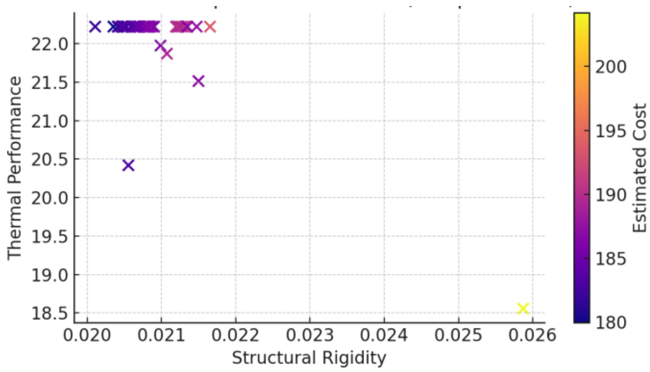

Fig. 6 Pareto Front Obtained Using a Genetic Algorithm for the Optimal Design of Construction Systems.

Similarly, the color of the dots reveals a cost distribution that tends to increase toward the extremes of the graph. Solutions with high stiffness or exceptional thermal performance tend to have the highest costs, consistent with the design logic that associates technical improvements with greater economic investment. However, the set of intermediate points includes options with high structural and thermal performance at moderate cost, making them optimal configurations for projects with budget constraints.

This analysis suggests that the application of evolutionary algorithms allows the efficient exploration of a complex and multidimensional solution space, facilitating the selection of construction strategies that simultaneously consider structural safety, thermal comfort, and economic viability. For future research, it is recommended to extend the evaluation model by incorporating criteria such as carbon footprint, life cycle analysis (LCA), and response to different seismic intensities.

The results of this study show that structural masonry has greater stiffness and dynamic symmetry than mixed masonry, which is consistent with the tests in [17], where progressive degradation was observed in URM walls under larger drifts, limiting the performance of RC-URM structures. In our case, the mixed masonry showed larger drifts in the Y-direction and higher accelerations in the upper floor, indicating a more flexible and less controlled response.

The modal distribution also reinforces these differences: structural masonry has higher natural frequencies, reflecting a more rigid and efficient dynamic behavior, in agreement with the results of [17]. In addition, [18] reports a hierarchical failure process in mixed HFM systems, with initial collapse of the masonry walls and subsequent deterioration of the frames. This pattern is related to the concentration of forces and drifts in the upper levels observed in mixed masonry. In addition, the phenomenon of "triple concentration" of shear forces pointed out by the authors is consistent with the uneven distribution of stiffness found in our simulations, highlighting the importance of considering damage and stiffness criteria in seismic design.

IV. Conclusions

The objective of this study was to compare the dynamic and seismic behavior of mixed masonry and structural masonry systems in low-rise buildings, evaluating their stiffness, displacements, and load distribution.

The results show that structural masonry provides greater stiffness, better drift control, and a more stable dynamic response. Mixed masonry showed lower overall displacements, but its response was more variable, especially in the Y-direction and at higher levels.

Modal analyses, level-by-level acceleration evaluations, and structural optimization using a genetic algorithm (GA) were performed, which allowed the identification of configurations with a good balance between stiffness, thermal efficiency, and cost.

Therefore, both systems are viable for low-rise housing. Structural masonry is suitable when stiffness and stability are priorities, while mixed masonry can be an option when material optimization is sought. The use of evolutionary algorithms such as GA allows for improved design by considering multiple criteria simultaneously.

Acknowledgment

The authors gratefully acknowledge Universidad Privada del Norte for its partial support of this research project.

References

[1] R. Vakilinezhad and S. Khabir, "Evaluation of thermal and energy performance of cool envelopes on low-rise residential buildings in hot climates," *Journal of Building Engineering*, vol. 72, Aug. 2023, doi: 10.1016/j.jobe.2023.106643.

[2] M. Santamouris *et al.*, "ON THE IMPACT OF URBAN CLIMATE ON THE ENERGY CONSUMPTION OF BUILDINGS," 2001. [Online]. Available: www.elsevier.com/locate/solener

[3] A. Sedaghat and M. Sharif, "Mitigation of the impacts of heat islands on energy consumption in buildings: A case study of the city of Tehran, Iran," *Sustain Cities Soc*, vol. 76, Jan. 2022, doi: 10.1016/j.scs.2021.103435.

[4] J. E. Daniell, B. Khazai, F. Wenzel, and A. Vervaeck, "The worldwide economic impact of historic earthquakes."

[5] C. Condori *et al.*, "Variable seismic anisotropy across the Peruvian flat-slab subduction zone with implications for upper plate deformation," *J South Am Earth Sci*, vol. 106, p. 103053, Mar. 2021, doi: 10.1016/J.JSAMES.2020.103053.

[6] C. M. Eakin, M. Obrebski, R. M. Allen, D. C. Boyarko, M. R. Brudzinski, and R. Porritt, "Seismic anisotropy beneath Cascadia and the Mendocino triple junction: Interaction of the subducting slab with mantle flow," *Earth Planet Sci Lett*, vol. 297, no. 3–4, pp. 627–632, Sep. 2010, doi: 10.1016/J.EPSL.2010.07.015.

[7] M. A. Gutscher, J. L. Olivet, D. Aslanian, J. P. Eissen, and R. Maury, "The 'lost inca plateau': cause of flat subduction beneath peru?," *Earth Planet Sci Lett*, vol. 171, no. 3, pp. 335–341, Sep. 1999, doi: 10.1016/S0012-821X(99)00153-3.

[8] RNE, "Reglamento Nacional de Edificaciones - RNE - Informes y publicaciones - Ministerio de Vivienda, Construcción y Saneamiento - Plataforma del Estado Peruano," gob.pe. Accessed: Apr. 24, 2025. [Online]. Available: https://www.gob.pe/institucion/vivienda/informes-publicaciones/2309793-reglamento-nacional-de-edificaciones-rne

[9] L. Bandeira Barros, M. Knockaert, and J. R. Tenório Filho, “Towards a more sustainable construction industry: Bridging the gap between technical progress and commercialization of self-healing concrete,” *Constr Build Mater*, vol. 403, p. 133094, Nov. 2023, doi: 10.1016/J.CONBUILDMAT.2023.133094.
[10] K. Kermeli *et al.*, “The scope for better industry representation in long-term energy models: Modeling the cement industry,” *Appl Energy*, vol. 240, pp. 964–985, Apr. 2019, doi: 10.1016/J.APENERGY.2019.01.252.
[11] S. Ozturk, “Optimization of thermal conductivity and lightweight properties of clay bricks,” *Engineering Science and Technology, an International Journal*, vol. 48, p. 101566, Dec. 2023, doi: 10.1016/J.JESTCH.2023.101566.
[12] Z. Wang, Q. Wang, and T. Ai, “Comparative study on effects of binders and curing ages on properties of cement emulsified asphalt mixture using gray correlation entropy analysis,” *Constr Build Mater*, vol. 54, pp. 615–622, Mar. 2014, doi: 10.1016/j.conbuildmat.2013.12.093.
[13] Ministerio de Vivienda, Construcción y Saneamiento, Norma Técnica E.030: Diseño Sismorresistente, Lima, Perú, 2018.
[14] Z. Yang and W. Z. Lu, “Prefabricated beam-slab structure optimization based on multi-layer graphical representation and genetic-RAO algorithm,” *Advanced Engineering Informatics*, vol. 64, p. 103050, Mar. 2025, doi: 10.1016/J.AEI.2024.103050.
[15] H. Lv, L. Yi, Z. Zhu, S. Dong, L. Shao, and X. Wu, “Prestress state, parametric analysis study and genetic algorithm-based tentative design of a novel pentagonal cable dome structure with tri-strut layout,” *Thin-Walled Structures*, vol. 208, p. 112815, Mar. 2025, doi: 10.1016/J.TWS.2024.112815.
[16] Z. Shen, J. Wu, and Y. Cao, “A dual-adaptive directed genetic algorithm for construction scheduling,” *Journal of Building Engineering*, vol. 96, p. 110659, Nov. 2024, doi: 10.1016/J.JOBE.2024.110659.
[17] A. Paparo and K. Beyer, “Quasi-static cyclic tests of two mixed reinforced concrete–unreinforced masonry wall structures,” *Eng Struct*, vol. 71, pp. 201–211, Jul. 2014, doi: 10.1016/J.ENGSTRUCT.2014.04.002.
[18] J. Zhang, X. Guo, X. Liu, and F. He, “Seismic performance of hybrid RC frame-masonry structures based on shaking table testing,” *Eng Struct*, vol. 333, p. 120174, Jun. 2025, doi: 10.1016/J.ENGSTRUCT.2025.120174.